DIFFUSIVE PROPERTIES OF WATER IN *ARTEMIA* CYSTS AS DETERMINED FROM QUASI-ELASTIC NEUTRON SCATTERING SPECTRA

E. C. TRANTHAM AND H. E. RORSCHACH
Rice University, Houston, Texas 77251

J. S. CLEGG
University of Miami, Coral Gables, Florida 33124

C. F. HAZLEWOOD
Baylor College of Medicine, Houston, Texas 77030

R. M. NICKLOW AND N. WAKABAYASHI
Oak Ridge National Laboratory, Oak Ridge, Tennessee 37830

ABSTRACT Results have been obtained on the quasi-elastic spectra of neutrons scattered from pure water, a 20% agarose gel (hydration four grams H_2O per gram of dry solid) and cysts of the brine shrimp *Artemia* for hydrations between 0.10 and 1.2 grams H_2O per gram of dry solids. The spectra were interpreted using a two-component model that included contributions from the covalently bonded protons and the hydration water, and a mobile water fraction. The mobile fraction was described by a jump-diffusion correlation function for the translation motion and a simple diffusive orientational correlation function. The results for the line widths $\Gamma(Q^2)$ for pure water were in good agreement with previous measurements. The agarose results were consistent with NMR measurements that show a slightly reduced translational diffusion for the mobile water fraction. The *Artemia* results show that the translational diffusion coefficient of the mobile water fraction was greatly reduced from that of pure water. The line width was determined mainly by the rotational motion, which was also substantially reduced from the pure water value as determined from dielectric relaxation studies. The translational and rotational diffusion parameters were consistent with the NMR measurements of diffusion and relaxation. Values for the hydration fraction and the mean square thermal displacement $\langle u^2 \rangle$ as determined from the Q-dependence of the line areas were also obtained.

INTRODUCTION

Water is the most abundant molecule in biological systems, ranging from ~50% to 90% by weight in most organisms, tissues, and cells, depending on the physiological state. The role of water in biological systems has been a subject of controversy; however, its role in biochemical and biological processes is certainly one of the most important unsolved problems in biology (1). The controversy arises in part from the lack of fundamental knowledge of the microscopic structure of pure water and water in biological systems. It also arises from the fact that the results of measurements with the various technologies used to study the properties of water in biological systems have not been consistently integrated with one another and with any reasonable model of water structure and dynamics.

The physical models used to describe the behavior of water in biological systems range from a simple bound-free exchange model (2–4) to the polarized multilayer hypothesis of Ling (5–10). Although experiments have been performed to test these views, no general consensus has emerged. In this paper, we review the NMR experiments on biological water, compare their results with those obtained from neutron scattering, and show that neutron scattering gives new results not obtainable by other methods.

MEASURING METHODS

Neutron Scattering Technique

The technique of quasi-elastic neutron scattering (QNS) is a powerful method for studying the nonperiodic (diffusive) motion of atoms in solids and liquids (11, 12). The results of QNS spectra measurements are usually interpreted within the framework of the Van Hove theory (13, 14), which relates the scattering law $S(Q,\omega)$ to the space-time

Dr. Wakabayashi's present address is the Department of Physics, Keio University, Hiyoshi, Yokohama, Japan 223.

correlation function $G(\mathbf{r},t)$ of the scattering particles. This correlation function can be calculated for various models for the assumed motion of the diffusing particles (e.g., Brownian, jump-diffusion, and oscillatory diffusion). The shape of the expected QNS spectra can be determined from the correlation function, and the parameters of the models determined by a fit to the experimental spectra. These parameters can then be related to the microscopic properties of the environment of the scattering atoms, (e.g., residence time, jump length, and rotational diffusion coefficient).

This method holds special promise for the study of the properties of water in biological systems. The structure of pure water can be studied with x-rays (15, 16), but these methods cannot be easily extended to noncrystalline biological systems, due to their heterogeneous molecular composition. Nuclear magnetic resonance (NMR) techniques have been extensively used to study the properties of water by measurement of the various relaxation times and the translational diffusion coefficient (3). The NMR relaxation parameters are determined by the environment of the proton moments (dipole-dipole interactions with other protons, located on other water molecules or within the cellular macromolecules) (17, 18), and the diffusive properties are determined by the intermolecular interactions as well as by the interaction with the biomolecular structures which can form obstructions and barriers for diffusion (19).

NMR measurements on the properties of water in biological systems have not yet provided a clear picture of the microscopic disposition of water within the cell. This is due to the heterogeneous character of the cell as well as to the fact that a single NMR measurement is carried out over a period of time, t, of the order of a few milliseconds or more (20–22). During this measuring time, the water molecules are diffusing within the cell, and their NMR parameters are determined by averages over distances $\sqrt{2Dt} \simeq 1$ μm where D is the diffusion coefficient of water. An interpretation of the results requires a detailed modeling of the heterogeneous environment of the cell, and there has not been universal agreement on the essentail features of such a model.

The QNS method gives information on the properties of the scattering atoms that depends directly on the microscopic environment of these atoms. The correlation function for the atomic motion is explored over a space domain on the order of a few ångströms and for $t \sim 10^{-12}$ s. The positional correlation of the atom determines the scattering. This is to be contrasted with the NMR measurements that give information on the correlation function for the orientation of the protonic moments (23).

In this paper, we present QNS spectra for water, an agarose gel, and four hydrations of *Artemia* cysts. The spectra are composed of two components, one that is elastic within the spectrometer resolution and another that is broadened by the diffusive motion. These spectra have been interpreted with diffusive correlation functions for the translational and rotational motion of the mobile water, and hydration (or "bound") fractions have been determined from an analysis of the line areas.

Sample Preparation

The water used for the preparation of all samples was double distilled and deionized. The pure water sample was contained in an aluminum sample chamber.

Agarose gel is a polymer $(C_{12}H_{18}O_9)_n$ of known structure (24). It contains 4 OH groups and 14 covalently bonded protons in each repeat unit. It was selected for a pilot study to determine if the spectrometer resolution was sufficient to separate the quasi-elastic line due to water protons from the elastic line of the polymer protons. In addition, NMR data on the diffusion coefficient and relaxation times have been published (25). Gels of 20% agarose by weight in water and deuterium oxide were prepared as follows. The appropriate amounts of de-ionized, distilled water or deuterium oxide, and electrofluorescence grade agarose powder were weighed, and then mixed in a small beaker. The sample was then covered and heated to 90°C in a water bath and maintained between 85° and 95°C for 30–60 min. The samples were then poured into preheated aluminum sample holders and allowed to set at room temperature for a minimum of 12 h before placing them in the spectrometer.

The cysts of *Artemia*, a primitive crustacean called the brine shrimp, consist of an inner mass of ~4,000 eucaryotic cells surrounded by a complex noncellular shell. Their ultrastructure, biochemistry, and physical properties have been described in some detail (26), and they have been used for the study of a wide variety of biological problems. Their utility for studies on cellular water arises from the ability of these cysts to undergo virtually complete dehydration in a reversible way (27) and to tolerate the conditions necessary to carry out the QNS study (28). The cysts used in these experiments were purchased from San Francisco Bay Brand, Inc. (Menlo Park, CA.) Approximately 90 ± 3% of this population, after processing, produced viable larvae when incubated at 25°C in seawater for 72 h. Large quantities of cysts were prepared by a thorough washing procedure carried out at 2–4°C, to suppress metabolic activity (29). The cysts were then dried at room temperature, separated by size (average diameter ~200 μm) and stored in a desiccator over $CaSO_4$ until used.

Various water contents (hydrations) were achieved by allowing the cysts to equilibrate with NaCl solutions of different concentration. The cysts were immersed overnight at 0°C. Because the inner shell of the cyst is impermeable to NaCl (28), the amount of water taken up is determined strictly by water activity of the NaCl solution. By this procedure, hydrations between 0.1 and 1.2 grams of H_2O per gram of dry cyst (g/g) were obtained. Maximum cyst hydrations are ~1.4 g/g, at which the cellular water content is ~1.7 g/g (~63% by weight). Details of hydration methods have been published (29).

The cysts were removed from solution and the surface water removed quickly. They were allowed to equilibrate with each other for 30–60 min in a closed vial; then they were transferred to an aluminum sample chamber for QNS measurements. A sample was also taken for preliminary determination of their water content by gravimetric procedures. (Drying was carried out at 100°–105°C for at least 6 h.) A final value of the water content was obtained from measurements on cysts taken from the sample chamber after the QNS experiment was completed. The two hydration values were always in close agreement, showing that cyst hydration was constant during the course of the experiment. Hatching tests showed that the viability before and after neutron exposure was the same as for controls that had not been exposed. Thus, exposure to neutrons had no effect on viability, and the results can be regarded as those for living intact cells.

Neutron Spectrometer

All of the spectra reported in this paper were taken on a triple-axis spectrometer (labeled HB2) at the High Flux Isotope Reactor (HFIR) at Oak Ridge National Laboratory. In these experiments, the monochromator and analyzer were pyrolytic graphite [(002) reflection]. Neutrons from higher-order reflections were removed with a beryllium filter. The analyzer was oriented to accept neutrons with an energy of 0.95 THz (~3.9 meV), and the neutron energy transfer was scanned by scanning the diffraction angle of the monochromator. Collimators with an angular full width at half-maximum of 20 min of arc were placed before and after the sample. The resolution function was determined from a run on a vanadium sample and was Gaussian with a full width at half maximum of 0.025 THz. The spectrometer scans were controlled by a PDP-8 computer. (Digital Equipment Corp., Marlboro, MA).

The intensity of the scattered beam was determined with a ^{3}He detector, interfaced with the computer. The counting time was determined by a low efficiency (uranium) fission detector that monitored the intensity of the incident beam. The data consisted of a print-out of the number of scattered neutrons obtained in the ^{3}He detector at each value of momentum and energy transfer during the time required to obtain a preselected number of monitor counts.

The sample holders were made from a standard aluminum alloy (2024), and they were machined so as to provide a sample chamber either 1 or 2 mm in thickness, and with lateral dimensions ~4 cm × 4 cm. The front and back covers had a thickness of 1 mm, and the chambers were sealed with indium wire gaskets and aluminum nuts and bolts. The beam

(~2.5 × 2.5 cm) always passed symmetrically through the sample chamber.

The thickness of the sample chambers was 1 mm for the pure water sample and for the agarose-H_2O gel. It was 2 mm for the agarose-D_2O gel and the brine shrimp cysts. These thicknesses were chosen so as to make the thickness, measured as a fraction of a neutron mean free path, roughly equal to 1/2 for all samples, which gives a transmission of ~60%. (The mean free path of neutrons in pure water is ~2 mm.)

The wavelength of the 0.95 THz neutrons used in these experiments was not sufficiently long to avoid all coherent reflections from aluminum. Reflection from the $\langle 111 \rangle$ planes was possible at a Bragg angle of $\theta = 79°$. The fraction of the beam scattered from this reflection was estimated to be ~3.5%, which would then have to be scattered by the water at rather large Q-values to contribute to the QNS spectra. We estimate that these neutrons make a small contribution to the background, but do not otherwise affect the spectra. All data were collected with the samples at the temperature of the spectrometer bay, which was $T = 21° \pm 1°C$.

DATA

Because the thicknesses of the various samples were adjusted to be roughly one-half a neutron mean free path, the number of counts from the different samples for each momentum transfer $\hbar Q$ and energy transfer $\hbar\omega$ were roughly the same for a given monitor setting. Approximately 100–400 counts per point were obtained in the far wings of the spectra, where the background and inelastic scattering are dominant, and ~1,000–3,000 counts were collected at the peak of the quasi-elastic line.

The spectral scans were usually taken at five Q values: $Q = 0.7$, 1.0, 1.2, 1.5, and 1.9 $Å^{-1}$ and for ~40 values of energy transfer $\hbar\omega$ between ±0.200 THz. One scan was taken of the *Artemia* cysts of hydration 1.2 g/g at $Q = 0.5$ A^{-1}. The separation of points near the quasi-elastic peaks was $\Delta\omega = 0.005$ THz. The samples from which spectra were obtained and the hydration of these samples are presented in Table I. Spectra were also obtained on an agarose-D_2O gel whose hydration level was adjusted so that the agarose content in mole percent was equal to that of the agarose-H_2O gel.

Typical raw data for the H_2O and D_2O agarose gels as obtained from the computer print-out are shown in Fig. 1. The number of counts as a function of energy transfer for $Q = 1.2$ $Å^{-1}$ is shown. The broadening for the H_2O gel that is due to the mobile water is evident.

TABLE I
WATER CONTENT OF NEUTRON SCATTERING SAMPLES

Sample	Hydration gm H_2O/gm dry solids
H_2O	∞
Agarose gel	4.0
Brine shrimp cysts	1.2
	0.78
	0.31
	0.10

ANALYSIS AND RESULTS

Models for Pure Water

In liquids such as water where atoms are associated with nearest neighbors by hydrogen bonds, the translational motion of the atoms is often described by a "jump-diffusion" model, which gives a Lorentzian scattering law (11, 12):

$$S_t(Q,\omega) = \frac{\Gamma_t(Q)}{2\pi} \frac{\exp(-Q^2\langle u_m^2\rangle)}{\omega^2 + \left(\frac{\Gamma_t(Q)}{2}\right)^2} \quad (1)$$

where $\hbar Q$ is the momentum change of the scattered neutron, $\Gamma_t(Q)$ is the full-width at half-maximum, and $\exp(-Q^2\langle u_m^2\rangle)$ is the Debye-Waller factor. One form of this model assumes that the molecules perform oscillations at quasi-equilibrium positions for a time τ, and that they then diffuse to a new position during the time τ_1. If $\tau_1 \ll \tau$, then

$$\Gamma_t(Q) = 2\{Q^2D + [1 - \exp(-Q^2\langle u_m^2\rangle)]/\tau\}/(1 + Q^2D\tau). \quad (2)$$

The mean square jump length is $\langle l^2\rangle \equiv 6\,D_1\tau_1$, D_1 is the diffusion coefficient during τ_1, and $D = (1/6)(\langle l^2\rangle/\tau) + \langle u_m^2\rangle/\tau$ is the macroscopic diffusion coefficient.

A modification of this model (30, 31) in which the diffusion during time τ_1 is replaced by an instantaneous jump to a new site at a distance l, and the oscillations treated with the Gaussian approximation, gives the width

$$\Gamma_t = 2Q^2D/(1 + Q^2D\tau), \quad (3)$$

provided that the probability $p(l)$ for a jump of length l is $p(l) \propto l\exp(-l/l_0)$. The macroscopic diffusion coefficient is $D = l_0^2/\tau = \langle l^2\rangle/6\tau$.

Eqs. 2 and 3 can both be fitted to the data over the Q range that can be easily studied, but there are some reasons to prefer Eq. 3 (30, 31). Because Eq. 3 has fewer parameters, we have adopted Eq. 3 for the interpretation of our data.

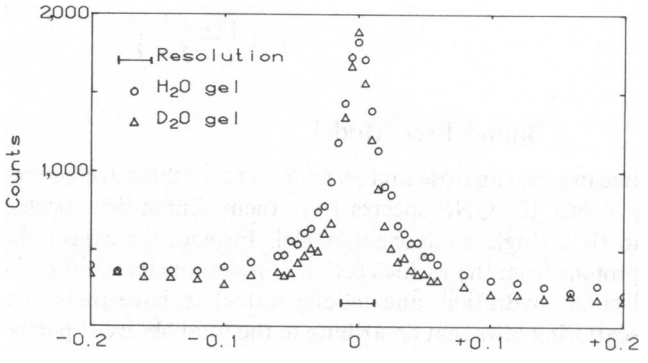

FIGURE 1 Neutron spectra at $Q = 1.2$ A^{-1} for a 4 g/g gel of agarose. ○, D_2O gel; △, H_2O gel. The spectrometer resolution function is Gaussian, with width shown.

The jump-diffusion model does not take the rotational motion of the water molecule into account, and it may seem surprising that its use leads to diffusive parameters in good agreement with measurements of the translational diffusion by other methods (e.g., tracer, NMR). Springer suggests (reference 11, p. 46) that the rotational motion in bulk water has a negligible effect on the line widths, since the reorientational correlation time is several times larger than the residence time τ of the jump-diffusion model, so the line width is determined principally by the translational motion. (This will be considered further in the Discussion section.) Irish et al. (32) have shown that the rotational motion makes a significant contribution to the line width at 1°C but does not contribute to the width at 22°C.

To assess the importance of the rotational motion to our measurements, we have adopted a scattering law for the rotational contribution based on the following assumptions: (*a*) The rotational and translational motions are uncorrelated, so that the Gaussian approximation holds (reference 14, pp. 375 ff.) (*b*) The scattering law $S_t(Q,\omega)$ for the translational motion is given by the jump-diffusion model, Eqs. 1 and 3. (*c*) The scattering law $S_r(Q,\omega)$ for the rotational motion is given by a rotational diffusion model in which the orientation of the molecular axes undergoes Brownian motion described by a rotational diffusion coefficient D_r (reference 11, pp. 66, 67):

$$S_r(Q,\omega) = j_0^2(Qa)\,\delta(\omega) + 3j_1^2(Qa)\frac{\Gamma_r/2}{\omega^2 + \left(\frac{\Gamma_r}{2}\right)^2} + (\text{higher terms}) \quad (4)$$

where $j_n(z)$ is a spherical Bessel function of the first kind; a is the molecular "radius"; $\Gamma_r = 4D_r$; $\delta(\omega)$ is the Dirac delta function; and the higher terms will be neglected.

The resulting scattering law $S_m(Q,\omega)$ is the convolution of S_r with S_t:

$$S_m(Q,\omega) = \frac{1}{2\pi}\frac{j_0^2(Qa)\Gamma_t \exp(-Q^2\langle u_m^2\rangle)}{\omega^2 + (\Gamma_t/2)^2} + \frac{3}{2\pi}j_1^2(Qa) \cdot \frac{(\Gamma_r + \Gamma_t)\exp(-Q^2\langle u_m^2\rangle)}{\omega^2 + \left(\frac{\Gamma_r + \Gamma_t}{2}\right)^2}. \quad (5)$$

Bound-Free Model

Because the agarose and *Artemia* cyst systems are heterogeneous, the QNS spectra from them cannot be expected to fit a single component model. Instead, we expect the protons from the various cellular environments (macromolecular, hydration, and mobile water) to have their own scattering laws that contribute to the total observed partial differential cross section.

The simplest model that takes into account the heterogeneity of these complex systems is one in which there are two phases of water. If we assume that one of these phases corresponds to water of hydration, which is tightly bound to macromolecules and structures within these systems, then we expect the protons in this phase to scatter nearly elastically. For convenience, we will henceforth refer to water whose quasi-elastic line width is small compared with the spectrometer resolution as bound water. This means only that its diffusional motion is $\lesssim 4$ times slower than pure water. This bound fraction may, however, be undergoing some high-frequency oscillations as in a solid, so there will be a Debye-Waller Q dependence to the intensity of this component. We assume that this component has the scattering law: $S_b(Q,\omega) = \exp(-Q^2\langle u_b^2\rangle)\delta(\omega)$.

The second component is assumed to be mobile and to diffuse with a scattering law given by Eq. 5. Because this phase may still be affected in some way by the presence of the other components of the system, we will not assume that the free parameters in Eq. 5 are the same as those found for pure water. If p is the fraction of the water that is in the bound phase, then the total scattering law is given by $S(Q,\omega) = pS_b(Q,\omega) + (1-p)S_m(Q,\omega)$.

The width of the quasi-elastic line given by Eq. 5 is on the order of the spectrometer resolution. Therefore, the observed partial differential cross section will be the convolution of the "ideal" partial differential cross section with the resolution function for the spectrometer. Because the measured resolution function is Gaussian, the observed line shape will be a Gaussian plus two Gaussian-Lorentzian convolutions:

$$S_{obs}(Q,\omega) = A_b G(\omega) + A_m G(\omega) * [L_t(\omega) + L_{r+t}(\omega)]$$

where

$$G(\omega) = \exp[-(\omega/\alpha)^2],$$
$$L_t(\omega) = 1/(1 + (\omega/\Gamma_t)^2$$
$$L_{r+t}(\omega) = 1/\{1 + [\omega/(\Gamma_r + \Gamma_t)]^2\}$$

and

$$G(\omega) * L(\omega) \equiv \int G(\omega')L(\omega - \omega')\,d\omega'.$$

Results for Pure Water

The number of counts as a function of ω at each value of Q were fitted with a function given by $F(\omega) = a\omega + b + A \cdot G(\omega) * L_t(\omega)$ where $a\omega + b$ represents the background. (The rotational contribution to the line was neglected; this will be taken up in the Discussion section.) The fitting was performed with a generalized least-squares search routine. The algorithm is Marquardt's search technique (33), which combines the best aspects of the Taylor's series (Newton-Raphson) method and the gradient search method (34). Four parameters were varied: a, b, A, and the width Γ of $L_t(\omega)$. Values of χ^2 per degree of freedom were in the range 0.85 to 1.05. The area of the Lorentzian component followed a Debye-Waller dependence as

described in Eq. 1. The mean-square thermal displacement $\langle u_m^2 \rangle$ was 0.33 Å^2. These data are plotted in Fig. 2. This value of $\langle u_m^2 \rangle$ is in good agreement with the results of other workers (35). (Some investigators [see reference 12, p. 349] prefer to call $6\langle u_m^2 \rangle$ the mean-square thermal displacement.) It should be noted that the range of values that have been reported for $\langle u_m^2 \rangle$ is quite large (reference 12, p. 349), and there is not always good agreement between QNS results and other methods.

The full width at half maximum Γ is plotted in Fig. 3. The data were fit with the model given by Eqs. 1 and 3, with the results $D = 2.4 \times 10^{-5}$ cm^2/s and $\tau = 1.2 \times 10^{-12}$ s. The fitted line in Fig. 3 is a plot of Eq. 3 with these parameters for pure water. The self-diffusion coefficient (D) is in good agreement with the results of other workers using QNS and other methods (11, 12, 36). The value of $\tau \simeq 10^{-12}$ s agrees with other QNS results (11, 12).

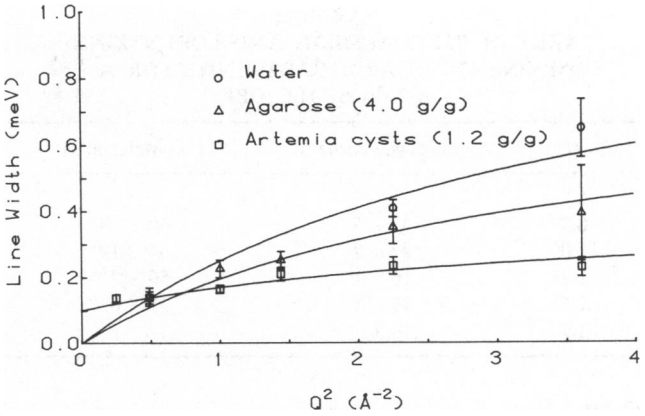

FIGURE 3 Line width Γ (in millielectron volts) vs. Q^2 (in reciprocal Ångströms squared) for pure water, the 4 g/g agarose-H_2O gel and the 1.2 g/g/ *Artemia* cysts. Water data for $Q^2 < 2$ Å^{-2} have been omitted. The curves drawn through the data are obtained from diffusion models and parameters described in the text.

Results for Agarose

The agarose polymer contains a significant number of chemically bonded protons. To separate the contribution of the agarose protons from the water, one can take advantage of the appreciably lower cross section of deuterium oxide compared with water. As described in the Measuring Method section, gels of agarose in water and agarose in deuterium oxide were prepared. The latter gel was used to determine the contribution of the agarose protons to the QNS spectrum.

The deuterium oxide gel data could also be fitted with a Gaussian plus a Gaussian-Lorentzian convolution, where the Gaussian had the width of the spectrometer resolution. The full fitting function was of the form $F(\omega) = a\omega + b + A \cdot G(\omega) + B \cdot G(\omega) * L_B(\omega)$. The amplitudes ($A$ and B) and the width of the Lorentzian L_B fully described the scattering from the agarose protons in the gels. The area of the Lorentzian contribution was of the same order as that of the Gaussian, and its presence was probably due to the motion of the OH side groups of the molecule.

The data obtained from the D_2O gel were used to remove the contribution of the agarose protons from the H_2O gel data. The parameters (amplitude and width) of the Lorentzian component of the D_2O gel, properly scaled according to agarose content, were used as fixed input parameters for the fits to the H_2O gel data. The Gaussian amplitude of the H_2O gel will contain a contribution of unknown amount from the bound water as well as a contribution from the agarose protons that is known from the measurements on the D_2O gel. The form of the fitting function for the water gels was thus: $F(\omega) = a\omega + b + A \cdot G(\omega) + B \cdot G(\omega) * L_B(\omega) + C \cdot G(\omega) * L_l(\omega)$, where B and L_B were fixed at values determined by the D_2O spectra, and the value of A contained contributions from the bound water and the agarose protons. The amplitude C of the Lorentzian due to the mobile water was ~1–5 times B, depending on the value of Q. The areas of the various contributions are given in Table II.

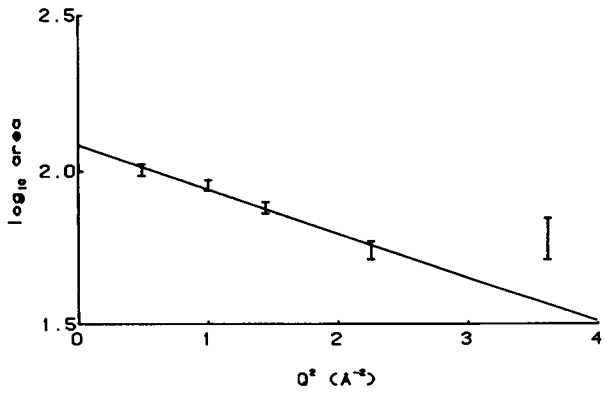

FIGURE 2 Debye-Waller plot for pure H_2O: area vs. Q^2. The slope gives the mean-square radius of the "thermal cloud" for the oscillatory motion of the protons.

To estimate the amount of bound and free water in the agarose gel the areas of the Gaussian and Lorentzian components at $Q = 0$ are used. The area as a function of Q will be called $S(Q)$, which is the integral of the scattering law $S(Q,\omega)$ over ω. At $Q = 0$ this area is proportional to the number of nuclei contributing to that portion of the spectrum (i.e., Gaussian or Lorentzian). If the scattering from the bound water had a Lorentzian contribution, as does the scattering from the agarose protons, these areas would not be strictly proportional to the corresponding number of nuclei. We do not have a good estimate of the size of this effect, but we believe it is not larger than ~10%.

Debye-Waller fits of the data of Table II were made to extrapolate back to the area at $Q = 0$. For the Gaussian component it was found that $S_g(0) = 39.8 \pm 7.0$ and $\langle u_b^2 \rangle = 0.37 \pm 0.13$ Å^2. (Note that $\langle u_b^2 \rangle$ characterizes the Gaussian contribution from the bound water and the agarose protons.) For the Lorentzian component, L_l, which is identified with mobile water, it was found that A_m =

TABLE II
AREA OF THE GAUSSIAN AND LORENTZIAN COMPONENTS IN ARBITRARY UNITS FOR A 20% AGAROSE-H_2O GEL

Q	Gaussian area	Lorentzian area
$Å^{-1}$		
0.7	37 ± 5	60 ± 19
1.0	27 ± 2	64 ± 10
1.2	16 ± 1	50 ± 7
1.5	19 ± 1	37 ± 6
1.9	14 ± 1	14 ± 5

$S_m(0) = 81 \pm 11$ and $\langle u_m^2 \rangle = 0.39 \pm 0.10$ Å^2. In the deuterium oxide gel it was found that $S(0) = 24.4 \pm 2.2$ for the Gaussian component. Therefore, the area due to bound water, A_b, is the difference between this area and the area of the total Gaussian in the water gel, and $A_b = 15.4 \pm 7.3$. The fraction of water that is bound is then $f_b = 0.160 \pm 0.066$. Another way of expressing the amount of bound water is in terms of the number of grams of water bound per gram of solid (i.e., the bound hydration, c). This was found by multiplying the bound fraction with the hydration (4 g water/g agarose). The bound hydration is $c = 0.64 \pm 0.26$, which is in good agreement with the value $c = 0.59$ quoted by Derbyshire and Duff (25).

The mean-squared thermal displacement for the mobile water was the same as that obtained for pure water, within experimental uncertainty. Another useful comparison between the mobile water and pure water is the dependence of the width Γ of the Lorentzian on Q^2, since this gives information about the diffusion parameters. This is shown in Fig. 3. The Lorentzian line width differs significantly from that of pure water for Q-values >1 Å^{-1}. The fact that the width for mobile water in agarose seems to be leveling off at a value significantly less than that of pure water indicates an increase of the residence time τ (see Eq. 3).

Results for Brine Shrimp

It is possible to hydrate the brine shrimp with deuterium oxide and maintain viability. However, it seems likely that substantial proton-deuteron exchange would occur in such a complex system, thus introducing uncertainties in the subtraction procedure. (Indeed, some exchange undoubtedly occurs in the agarose gels [37].) For this reason we did not attempt to measure the deuterium-water difference spectra as we did for the agarose. Instead, the scattering from the brine shrimp was studied as a function of hydration. The data were then fitted with a single Gaussian representing the elastic scattering of both water and solid protons, plus a single Gaussian-Lorentzian convolution representing the quasi-elastic scattering of both water and solid protons. From these data the contribution of the solids in the brine shrimp were estimated by extrapolating to zero hydration and then subtracting from the total

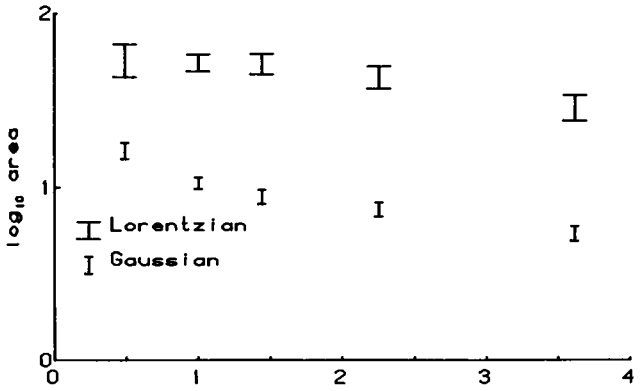

FIGURE 4 Debye-Waller plot for the Lorentzian and the Gaussian components for the 1.2 g/g *Artemia* cysts.

scattering. We identified the Gaussian component of the difference spectrum with bound water and the Lorentzian component with mobile water.

The areas of the Gaussian and Lorentzian components as a function of Q for brine shrimp for a hydration of 1.2 g/g are plotted in Fig. 4. The other hydrations gave similar results. For the Lorentzian component, the area appeared to be relatively independent of Q. To estimate the area of this component, the area for the lowest Q values were averaged together. The decision of how many Q values to use was made on the basis of visual inspection of the data for each hydration. The number of points averaged on the log area vs. Q^2 plots were 5, 4, 3, and 3 for the hydrations 0.10, 0.31, 0.78, and 1.2 g/g, respectively.

For the Gaussian component, the areas seemed to follow a Debye-Waller dependence on Q with an increase in slope as $Q \rightarrow 0$. If the low Q point was omitted, the areas could be fitted with a single Gaussian in Q. The percent of the QNS spectrum that was estimated to be in the Gaussian and Lorentzian components is shown in Table III.

The percent of the QNS spectrum in the Gaussian is plotted against the concentration of cyst water in Fig. 5. A straight line fits these data well, and indicates that 86 ± 1% of the QNS spectrum would be Gaussian if there were no water present in the sample. This allows us to estimate the

TABLE III
DISTRIBUTION OF THE QNS SCATTERING BETWEEN THE GAUSSIAN AND THE LORENTZIAN AT Q = 0 FOR THE ARTEMIA CYST

Hydration	% water by weight	Gaussian	Lorentzian
		%	%
0.10	9.1	78 ± 2	21.6 ± 0.7
0.31	23.7	65 ± 5	35.3 ± 0.8
0.78	43.8	48 ± 4	52 ± 4
1.20	54.6	38 ± 3	62 ± 5

If the low Q point is included in the analysis, the area of the Gaussian is increased by ~20%.

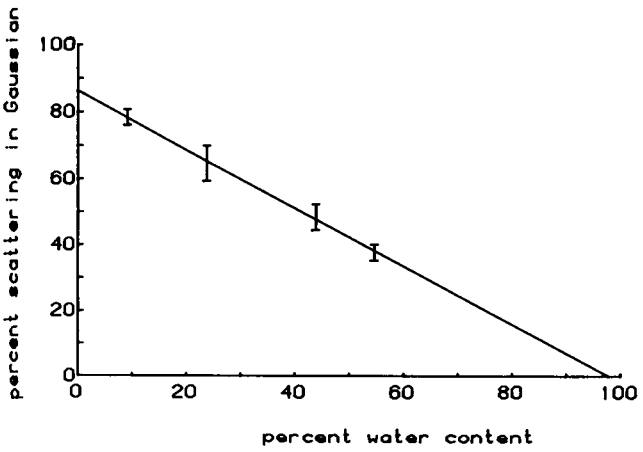

FIGURE 5 Percent area contained in the Gaussian component for *Artemia* cysts at $Q = 0$ vs. cyst hydration in grams per gram. Extrapolation to zero hydration gives 86% Gaussian contribution to the line area due to the solids.

distribution between the Gaussian and Lorentzian components for the brine shrimp, assuming that this distribution did not change as a function of hydration.

An elemental analysis of *Artemia* cysts shows (38) that for every gram of dry brine shrimp, there are 0.0801 grams of hydrogen. Because each gram of water contains 0.1119 grams of hydrogen, we can estimate the amount of scattering at each hydration that is due to the water and to the dry solids in the cysts. These estimates are shown in Table IV. The data are presented in terms of the percentage that is due to each component.

Table III gives the percent of brine-shrimp solid scattering that is Gaussian and Table IV the percent of the QNS scattering that is due to the brine shrimp solids. From these we could calculate the amount of scattering to expect in the Gaussian and Lorentzian components due to the brine-shrimp solids. We substracted these figures from the data in Table III to calculate the amount of the Gaussian scattering due to water and the amount of Lorentzian scattering due to water. When we identified the Gaussian component of water with bound water and the Lorentzian with mobile water, we could calculate the bound fraction, as was done for the agarose gels. In addition, from the hydrations and bound fractions the values of c was calculated. These results are given in Table V.

This technique of analyzing the data did not allow us to compare the Q dependence of the line width of the mobile water Lorentzian with bulk water, as was done for agarose in Fig. 3. This was because we had not separated the contributions of the solids and the water at every Q value. We had only separated the contributions at $Q = 0$. We can, however, examine the Q dependence of the width of the Lorentzian component found for the highest hydration. The previous analysis leds to an estimate that at $Q = 0$ the solids contributed only ~8% of the area of the Lorentzian. (37% of the scattering was due to the solids [Table IV], of

TABLE IV
PERCENT OF SCATTERING DUE TO EACH COMPONENT OF THE BRINE SHRIMP

Hydration	Solid scattering	Water scattering
g/g	%	%
0.10	87.74	12.26
0.31	69.78	30.22
0.78	47.85	52.15
1.20	37.36	62.64

which 14% was in the Lorentzian line [Fig. 5]. The Lorentzian contribution due to the solids was thus 5% of the total, or 8% of the Lorentzian contribution of 62% from the water plus solids of the hydrated brine shrimp.) If we assume that the Debye-Waller factors of the Lorentzian and Gaussian terms did not differ greatly so that this contribution did not change significantly as Q increased, then the Lorentzian will be dominated by the mobile water at all Q values. Fig. 3 shows the width $\Gamma(Q)$ of the Lorentzian for $h = 1.20$, without any correction for the contribution to the Lorentzian from the bound protons. The width of this Lorentzian deviates dramatically from that of pure water, since it is relatively independent of Q and approximately three times smaller than that of pure water at large Q. The data point at $Q = 0.5$ Å^{-1} was taken to confirm this behavior. The number of counts collected at this value of Q was increased to three times that collected at other Q values to reduce the statistical uncertainties. We did not take data at this low Q value for agarose or water, since the line became much narrower than the spectrometer resolution. However, the line from the *Artemia* cysts did not narrow. The line width vs. Q evidently cannot be well-described by the jump-diffusion model that is appropriate for pure water.

A determination of the Debye-Waller factor for the water in *Artemia* cysts at various hydrations was not possible due to the previously mentioned difficulty of subtracting the contribution from the solids at $Q \neq 0$. For $h = 1.2$ g/g, we can obtain a mean-squared displacement for the "Gaussian component" from Fig. 4, but the areas

TABLE V
PERCENT OF TOTAL SCATTERING DUE TO WATER COMPONENTS AND CALCULATED AMOUNT OF BOUND WATER IN THE BRINE SHRIMP

Hydration	Gaussian	Lorentzian	f_b	c
	%	%		
0.10	2.8 ± 2.5	9.5 ± 0.7	0.23 ± 0.16	0.023 ± 0.016
0.31	4.5 ± 5.4	25.7 ± 0.8	0.15 ± 0.15	0.046 ± 0.047
0.78	7.2 ± 4.0	45 ± 4	0.14 ± 0.07	0.11 ± 0.05
1.20	5.5 ± 2.5	57 ± 5	0.09 ± 0.04	0.11 ± 0.04

Although the statistical errors are large, there is some indication that the bound hydration c varies with hydration, being smaller at the lower hydrations.

for this component contained a substantial (~50%) contribution from the protons in the solid as well as the contribution from the bound water. We could not determine a value for the mean-squared displacement of the mobile water, since the rotational motion must be considered, as described in the next section. A comparison of the mean-squared displacements for water, 20% agarose, and 1.2 g/g brine shrimp is given in Table VI.

DISCUSSION

Rotational Contribution to the Scattering Law

The results presented in Analysis and Results for the diffusive properties of pure water and 20% agarose gel are based on a particular model for the protonic motion: the jump-diffusion model as expressed in Eqs. 1 and 3. The parameters [areas, $\Gamma(Q^2)$ and the derived quantities D and τ] obtained by fitting the experimental data to this model by the least-squares method, therefore cannot be regarded as really fundamental, since they are model dependent. Nevertheless, we believe that the comparisons made between the systems have validity beyond this particular model, since we have consistently applied the same model in the same way.

In the analysis of our data, we used only a single Lorentzian to fit the scattering law given by Eq. 5. This scattering law consists of two Lorentzian lines L_t and L_{r+t} of different widths. In the case of water, the influence of the second line, L_{r+t}, which was broadened by the rotational motion, lead to a small increase in the width obtained by a least-squares fit of the data with a single Lorentzian. At low Q, where the translational line was narrow, the relative amplitude of the rotationally broadened line was small, while at high Q, the translational line was very broad, so that the widths of the two lines were more nearly the same. Calculations based on this model with a value of $D_r = 8 \times 10^{10}$ s^{-1} for pure water (see Discussion section on Comparison with NMR) showed that the net result was that the measured line was broadened by ~4% at $Q = 0.5$ A^{-1}, increasing to ~15% at $Q = 1.9$ A^{-1}. This broadening was significant at high Q, but not much outside the error bars of our measurements.

The same conclusions hold for agarose. Previous results (25) have shown that the NMR measured diffusion coefficient D_{nmr} in a 20% agarose gel is reduced to ~0.62 D_o, where D_o is the value for pure water. A portion of this reduction can be ascribed to obstructions. If it is assumed that the polymers in the gel are equivalent to an ordered array of cylinders, then the obstruction effect can be estimated by (19, 39, and Rorschach and Hazlewood, unpublished data)

$$D_{nmr} = \frac{D(\text{agarose})}{1 + 0.8\phi}(1 - f_B),$$

where D(agarose) is the "local" diffusion coefficient in agarose, ϕ is the volume fraction of the cylinders (solids), and f_B = bound fraction = 0.16. For $\phi = 0.2$, we find D(agarose) = 0.8 D_o. A calculation of the influence of the rotational motion on the agarose line width can now be made, as we did above for pure water. If we assume a rotational diffusion coefficient equal to that of pure water, we find a broadening of the measured line by ~4–20%, depending on the value of Q. This calculation probably overestimates the broadening, since it is likely that the rotational diffusion coefficient is considerably less in the agarose gel, which would greatly reduce the broadening caused by the rotational contribution. This will be considered further in the Discussion section on Comparison with NMR.

The *Artemia* results, in contrast, can only be understood by taking the rotational motion into account, since the translational diffusion coefficient was greatly reduced from that of pure water. Previous NMR measurements in *Artemia* (39) show that the diffusion coefficient was reduced by a factor of 7 for a hydration of 1.2 g/g. Some of this reduction may be due to the presence of diffusion barriers (e.g., membranes and macromolecular structures). Indeed, the pulsed-field-gradient measurements of Tanner (40, 41) show that approximately one-half of the reduction was due to barriers, leaving an estimated reduction of 3.5 for the "local" diffusion coefficient. Such a greatly reduced value for D will have a strong influence on the observed neutron scattering. In fact, the translational line will now be much narrower than the spectrometer resolution, and it will be included with what we have termed bound water in our analysis. The observed Lorentzian line will be the rotationally broadened term (the second term of Eq. 5), and the observed width will be $\Gamma_r + \Gamma_t$. The diffusion parameters obtained from this analysis, based on Eq. 5, are presented in Table VII. The curves drawn through the data points in Fig. 3 are fits with these parameters.

The Q-dependence of the area of the Lorentzian line (see Fig. 4) is not inconsistent with this analysis. According to Eq. 5, the area should be proportional to $j_1^2(Qa)\exp(-Q^2\langle u_m^2\rangle)$. This factor approaches zero as $Q \to 0$, but it

TABLE VI
MEAN-SQUARED DISPLACEMENTS FOR THE GAUSSIAN (ELASTIC) AND LORENTZIAN (QUASI-ELASTIC) CONTRIBUTIONS FROM THE LISTED SCATTERERS

	$\langle u_b^2\rangle$ elastic	$\langle u_m^2\rangle$ quasi-elastic
	A^2	A^2
Pure Water	—	0.33 ± 0.02
H_2O in 4 g/g agarose	0.37 ± 0.3	0.39 ± 0.10
H_2O in 1.2 g/g brine shrimp	0.23 ± 0.03*	—

*Contains contributions from solids.

TABLE VII
DIFFUSION PARAMETERS USED TO FIT SCATTERING LAW TO QNS DATA*

System	D/D_0	τ/τ_0	D_r
			$10^9 S^{-1}$
Pure H_2O	1	1	—
20% agarose gel (4 g/g)	0.80	1.4	—
Artemia cyst (1.2 g/g)	0.29	3.9	6.0

*See Fig. 3.

has a very broad maximum at $Q \simeq 1$ A^{-1} for $\langle u_m^2 \rangle / a^2 = 1/2$ and $a \simeq 1$ A, and is relatively flat in the entire Q range of our experiments.

Multiple Scattering Corrections

A possible source of error in relating the line widths to the diffusive parameters through Eq. 3 is multiple scattering effects. Multiple scattering will alter the Lorentzian lineshape predicted by Eqs. 1 and 3, and least-squares fits to the line by a single Lorentzian will in general lead to a broader line than would be obtained from single scattering. The line area from which the Debye-Waller factor and hydration fractions are determined will also be affected. Multiple scattering effects have usually been ignored in quasi-elastic scattering experiments. This has been justified on the basis that measurements with different sample thicknesses give similar results, or that the effects are negligible in "sufficiently" thin samples (e.g., with transmissions ~90%), or that inelastic background subtraction compensates for it. Such arguments are dangerous, since the influence of multiple scattering depends on sample shape as well as on thickness, and the influence of sample shape on line areas may be appreciable.

The best way to determine the influence of multiple scattering is to calculate the scattering with a Monte-Carlo method. J. R. D. Copley has developed a program called MSCAT (42, 43) that calculates the observed scattering based on a theoretical scattering law and a sample geometry supplied by the user. We have used this program to determine the scattering due to the quasi-elastic portion of the spectrum for an experimental geometry similar to that used in this study. The scattering law described by Eqs. 1 and 3 was used with $D = 2.4 \times 10^{-5}$ cm^2/s and $\tau = 10^{-12}$ s. The "sample" used in the program was a 1-mm thick slab-shaped sample of pure water. Simulated data were obtained for this "sample" from the MSCAT calculation. These data were treated as experimental data, and our fitting routines were used to determine the effective areas and widths.

Fig. 6 illustrates the corrections to the width and integrated intensity which these calculations predict. The errors are on the order of 10% in the width and do not vary much with Q. The amplitude corrections are of the same order, except near $Q = 1.5$ A^{-1}, where they are considerably larger. There is no strong experimental evidence for the large decrease in area at $Q = 1.5$ A^{-1} (see Fig. 2), and we have made no corrections to any of our data for multiple scattering. Because all samples had nearly the same transmission, the correction would be roughly the same in all cases, so that, although the absolute values of the parameters derived from the widths and areas may be in error by ~10%, the relative values should be unaffected.

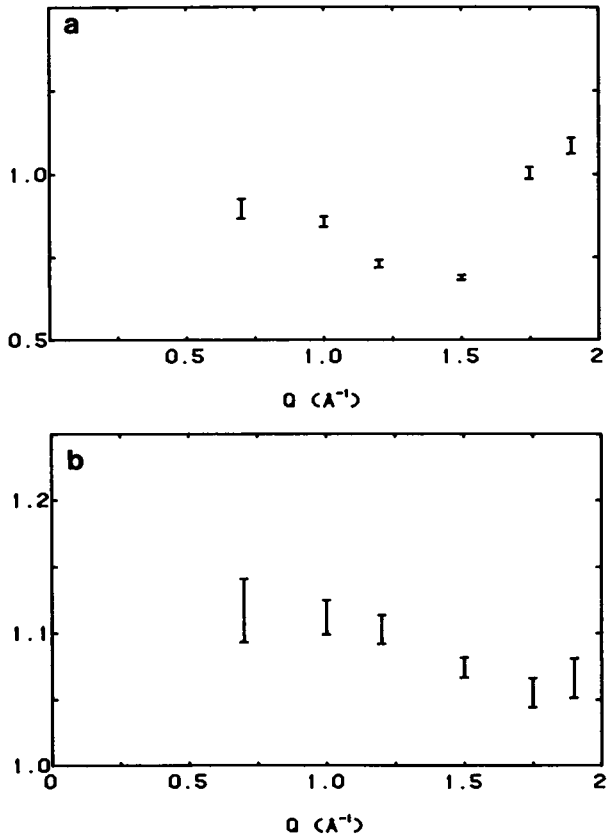

FIGURE 6 Multiple scattering correction for a 1-mm slab of H_2O as determined by a Monte Carlo calculation: (*a*) Ratio of line area with multiple scattering to that without multiple scattering vs. Q. (*b*) Ratio of line width with multiple scattering to that without multiple scattering vs. Q.

Comparison with NMR and Dielectric Relaxation Results

The present neutron scattering results combined with previous NMR data on agarose gels and *Artemia* cysts give new insight into the disposition and dynamics of the water in these systems.

Agarose Gels. The neutron scattering can be well described by a jump-diffusion model in which $D = 0.8\ D_0$, $\tau = 1.4\ \tau_0$ (D_0 and τ_0 are the values for pure water.) The line plotted in Fig. 3 was obtained from Eq. 3 with these parameters. This value for D is consistent with the NMR results on diffusion (25) and indicates that there is a "local" reduction in the values of D that cannot be associated with obstructions or barriers. This might not be

evident from the initial slope of $\Gamma(Q^2)$ in Fig. 3, but that conclusion is justified by the increased value of the residence time τ that is related to the diffusion coefficient by $6D\tau = \langle l^2 \rangle$, where $\langle l^2 \rangle$ is the mean-squared jump distance. The influence of the gel is thus to stablize the water structure without much change in average water-water distances but with an increased "binding" time between jumps.

The mean-square atomic displacement did not differ greatly from that of pure water (Table VI), which indicates that, although the residence time was increased due to association with the polymer chains, the local oscillatory motion, and therefore the binding forces experienced by the protons, were not much changed.

The NMR relaxation time T_1 has been measured by Woessner and Snowden (37) for agar gels and by Derbyshire and Duff (25) for agarose gels. Woessner and Snowden show that $(1/T_1)_{agar} = (1/T_0)^0 + 8.2\ C$ at 25°C, where C is agar concentration in grams per cubic centimeter of H_2O, and the zero superscript indicates the value for pure water. This gives a T_1 of 0.5 s for a 20% gel, in good agreement with an extrapolation of the reesults of Derbyshire and Duff, which gives $T_1 \simeq 0.4$ s for a 20% agarose gel, a reduction of a factor of ~6 from the value for pure water.

The T_1 value for the water in agarose gel contains contributions from both rotational and translational motion (23): $(1/T_1)_{agarose} = (1/T_1)_{rotational} + (1/T_1)_{translational}$. The rotational relaxation rate was determined by the rotational diffusion coefficient D_r and the translational relaxation rate by D. In the shortcorrelation time limit (23), $(1/T_1)_i \propto 1/D_i$. Thus, the 20% reduction in D will not produce the observed reduction in T_1. The value of D_r for the gel is unknown, but the analysis of the *Artemia* data in the next paragraph suggests that D_r may be considerably smaller in the gel than in pure water. If D_r were reduced by a factor of ~8, then the value of $T_1 = 0.5$ s could be explained as a bulk mechanism without invoking rapid exchange with a solidlike hydration layer. Such a reduction in D_r would also account for the good fit of the neutron scattering data to the jump diffusion model, since the rotational motion would then broaden the line by only a few percent. In this picture, T_1 would be due to bulk mechanisms, while T_2 would be determined by exchange with a solidlike phase whose correlation time is too long to affect T_1.

Artemia Cysts. The neutron scattering in this case can be well described by a combination of translational and rotational diffusion for which $D = 0.29\ D_0$, $\tau = 3.9\ \tau_0$, and $D_r = 6 \times 10^9\ s^{-1}$. The line plotted in Fig. 3 is $\Gamma(Q^2) = \Gamma_r + \Gamma_t$, where $\Gamma_r = 4D_r$ and Γ_t is given by Eq. 3, with these parameter values. This value of D is consistent with the NMR diffusion measurements (39), and shows that the large reduction in D is not entirely due to barriers or compartments, but is a true local effect due to the stabilizing of the water by the nonaqueous components present in these cells. The picture is very much the same as for agarose, except more pronounced due to the relatively higher concentration of solids in the *Artemia* system and a consequent larger reduction in D. The amount of intercellular surface area in living cells is indeed very large (3), so that the result is not surprising. The mean-square atomic displacement is considerably less than that of pure water, but this may be due to the large (~50%) contribution from the bound protons (see Table VI).

The value of D_r for *Artemia* can be compared with results from dielectric relaxation studies by Clegg et al. (44). The comparison is not entirely straightforward, since dielectric dispersion measurements do not measure D_r directly. Furthermore, the problem of exchange among the various fractions of water also needs careful consideration in interpretations of dielectric results.

Previous measurements on pure water (45) have shown that the Debye relaxation time τ_D is 0.93×10^{-11} s at 20°C. The "microscopic" relaxation time τ_μ is smaller, due to local field effects, and is (reference 45, p. 299) $\tau_\mu \simeq \tau_D/1.5$. The rotational diffusion coefficient is related to τ_μ by (23) $D_r = 1/2\ \tau_\mu$, and thus $D_r = 8.1 \times 10^{10}\ s^{-1}$ for pure water.

The value $D_r = 6 \times 10^9\ s^{-1}$ for *Artemia* measured by neutron scattering is lower than that of pure water by a factor of ~13. A similar increase in τ_D has been observed in systems of relatively low water content, such as hemoglobin (46, 47) and lysozyme (48). These changes are much larger than those obtained by Clegg et al. (44), who have measured the dielectric dispersion for water in *Artemia* cysts for frequencies up to 70 GHz. They find a relaxation time only slightly longer (~2 times) than that of pure water, which suggests D_r is reduced by a similar factor. Previous work on biological systems of higher water content (49) also reported values of τ_D close to that of pure water. Nevertheless, this is not convincing evidence that the water in the cell is predominantly "free" water. Should rapid exchange occur, the dielectric properties would be dominated by the presence of only a small fraction of free water, in the same way that the value of T_2 in biological systems is influenced by a small rapidly relaxing phase of water. Such considerations have not been taken into account in the analysis of microwave dielectric studies of water in cells and tissues (44, 49), and they may be important.

The above values for D and D_r obtained from the neutron spectra are also consistent with the NMR relaxation time T_1. The value of T_1 for cysts at 1.2 g/g water content is ~250 ms (50), a factor of ~12 less than that of pure water. For pure water, T_1 is determined by the rotational and translational motion (23)

$$\left(\frac{1}{T_1}\right)^0 = \left(\frac{1}{T_1}\right)^0_{\text{rotational}} + \left(\frac{1}{T_1}\right)^0_{\text{translational}},$$

where (51)

$$\left(\frac{1}{T_1}\right)^0_{\text{rotational}} \simeq 2\left(\frac{1}{T_1}\right)^0_{\text{translational}}.$$

The neutron results show that the rotational contribution to $(1/T_1)$ for *Artemia* cysts was ~13 times that for pure water, since the value of D_r was reduced by this factor. The translational contribution was increased by a factor of ~4. This gave an expected reduction factor in T_1 for *Artemia* of ~10, which agrees rather well with the observed values of T_1 (50).

CONCLUSIONS

We thus conclude that the neutron, NMR, and dielectric relaxation measurements on *Artemia* cysts are all consistent with a picture in which the majority of the cell water has strongly reduced translational and rotational diffusion coefficients that are not due to obstructions, compartments, or exchange with minor phases, but are instead an intrinsic feature of the intracellular water. This result supports hypotheses, such as those of Berendson (52) and Ling (5–10) that the motional freedom of water molecules is reduced by association with cellular macromolecules. The consequences of this conclusion could be far reaching, since much of current thought about cell structure and function considers the water to exhibit properties that are the same as those of bulk aqueous solutions. It seems very likely that the role of water in chemical reactions, protein conformations, ion exclusion, and other cellular functions will prove to be a more dynamic one than has heretofore been assumed (5–10, 53).

The authors wish to thank Dr. A. Callahan for the stimulus to initiate these neutron scattering experiments. We also thank D. Heidorn for assistance with the *Artemia* cyst measurements.

This research was supported in part by Office of Naval Research contracts N00014-79-C-0492 and N00014-76-C-0100, by Oak Ridge Associated Universities Participation Agreement S-2016, by R. A. Welch Foundation grant Q390, and by National Science Foundation grant PCM 79-25609. Oak Ridge National Laboratory is operated by Union Carbide under contract W-7405-eng-26 with the U. S. Department of Energy.

Received for publication 14 February 1983 and in final form 3 October 1983.

REFERENCES

1. Jardetzky, O., and N. C. Wade-Jardetzky. 1980. Nuclear magnetic resonance as a structural method in molecular biology. *In* Felix Bloch and Twentieth Century Physics. M. Chodorow, R. Hofstadter, H. E. Rorschach and A. L. Schawlow, editors. Rice University Studies, Houston, TX. 66:57–82.
2. Mathur-DeVré, R. 1979. The NMR studies of water in biological systems. *Prog. Biophys. Mol. Biol.* 35:103–134.
3. Drost-Hansen, W. and J. S. Clegg, editors. 1979. Cell-Associated Water. Academic Press, Inc., New York.
4. Kuchel, P. W. 1981. Nuclear magnetic resonance of biological samples. *Crit. Rev. Anal. Chem.* 12(3):157–331.
5. Ling, G. N. 1965. The physical state of water in living cell and model systems. *Ann. NY Acad. Sci.* 125:401–417.
6. Ling, G. N. 1970. The physical state of water in living cells and its physiological significance. *Int. J. Neurosci.* 1:129–152.
7. Ling, G. N. 1979. Hydration of macromolecules. *In* Water and Aqueous Solutions: Structure, Thermodynamics and Transport Processes. R. A. Horne, John Wiley and Sons, Inc., New York. 663–700.
8. Ling, G. N., editor. 1979. The polarized multilayer theory of cell water and other facets of the association-induction hypothesis concerning the distribution of ions and other solutes in living cells. *In* The Aqueous Cytoplasm. A. D. Keith, editor. Marcel Dekker, Inc., New York. 23–60.
9. Ling, G. N. 1981. Water and the living cell as seen from the viewpoint of a new paradigm. *In* International Cell Biology 1980-1981. H. G. Schwerger, editor. Springer-Verlag, Berlin. 904–914.
10. Ling, G. N., M. M. Ochsenfeld, C. Walton, and T. S. Bersinger. 1980. Mechanism of solute exclusion from cells: the role of protein-water interaction. *Physiol. Chem. Phys.* 12:3–10.
11. Springer, T. 1972. Quasi-elastic neutron scattering for the investigation of diffusive motions in solids and liquids. *Springer Ser. Modern Phys.* Vol. 64.
12. Page, D. I. 1971. The scattering of neutrons by liquid water. *In* Water. F. Franks, editor. Plenum Publishing Corp., New York. Vol. 1. 333–362.
13. Van Hove, L. 1954. Correlations in space and time and Born approximation scattering in systems of interacting particles. *Phys. Rev.* 95:249–262.
14. Marshall, W., and S. W. Lovesey. 1971. Theory of Thermal Neutron Scattering. Clarendon Press, Oxford University Press, Oxford.
15. Narten, A. H., M. D. Danford, and H. A. Levy. 1967. X-ray diffraction study of liquid water in the temperature range 4–200°C. *Discuss. Faraday Soc.* 43:97–107.
16. Narten, A. H., and H. A. Levy. 1972. Liquid water: scattering of x-rays. Water. F. Franks, editor. Plenum Publishing Corp., New York. Vol. 1. 311–332.
17. Edzes, H. T., and E. T. Samulski. 1978. The measurement of cross-relaxation effects in the proton NMR spin-lattice relaxation of water in biological systems: hydrated collagen and muscle. *J. Magn. Reson.* 31:207–229.
18. Koenig, S. H., R. G. Bryant, K. Hallenga, and G. S. Jacobs. 1978. Magnetic cross-relaxation among protons in protein solutions. *Biochemistry.* 17:4348–4358.
19. Cleveland, G. G., D. C. Chang, C. F. Hazlewood, and H. E. Rorschach. 1976. Nuclear magnetic resonance measurement of skeletal muscle. Anisotropy of the diffusion coefficient of the intracellular water. *Biophys. J.* 16:1043–1053.
20. Stejskal, E. O. 1972. Spin-echo measurement of self-diffusion in colloidal systems. *Adv. Mol. Relax. Interact. Processes.* 3:27–42.
21. Gross, B., and R. Kosfeld. 1969. Application of spin-echo method in measurement of self-diffusion. *Messtechnick.* 7/8:171–177.
22. Tanner, J. E. 1975. Self-diffusion in cells and tissues. Office of Naval Research Report NWSC/CR/RDTR-6, Division of Medical and Dental Science, Arlington, VA.
23. Abragam, A. 1961. The Principles of Nuclear Magnetism. Clarendon Press, Oxford University Press, Oxford. 289–305.
24. Noller, C. R. 1965. Chemistry of Organic Compounds. W. B. Saunders Co., Philadelphia, PA. 432 pp.
25. Derbyshire, W., and I. D. Duff. 1974. NMR of agarose gels. *Faraday Discuss. Chem. Soc.* 57:243–254.
26. Persoone, G., P. Sorgeloos, O. Rolls, and E. Jaspers, editor. 1980. The Brine Shrimp Artemia. Physiology, Biochemistry, Molecular Biology. Universa, Wetteren, Belgium. 2:1–664.
27. Clegg, J. S., A. C. Zettlemoyer, and H. H. Hsing. 1978. On the residual water content of dried but viable cells. *Experientia (Basel).* 34:734–735.

28. Clegg, J. S., and Z. P. Conte. 1980. A review of the cellular and developmental biology of *Artemia*. The Brine Shrimp Artemia. Physiology, Biochemistry, Molecular Biology. G. Persoone, P. Sorgeloos, O. Rolls, and F. Jaspers, editors. Universa, Wettern, Belgium. 2:11–54.
29. Clegg, J. S. 1978. Interrelationships between water and cellular metabolism in *Artemia* cysts. VIII. Sorption isotherms and derived thermodynamic quantities. *J. Cell. Phys.* 94:123–138.
30. Eglestaff, P. 1967. An Introduction to the Liquid State. Academic Press, Inc., New York. Chapt. 10. 118–132.
31. Cocking, S. J. 1969. Atomic motion in liquid sodium. I. Diffusive motion. *J. Phys. Ser. C.* 2:2047–2062.
32. Irish, J. D., W. G. Graham, and P. A. Egelstaff. 1978. Diffusive motion of water molecules near 1°C. *Can. J. Phys.* 56:373–380.
33. Marquardt, D. W. 1963. An algorithm for least-squares estimation of nonlinear parameters. *SIAM (Soc. Ind. Appl. Math.) J. Appl. Math.* 11:431–441.
34. Bevington, P. R. 1969. Data Reduction and Error Analysis for the Physical Sciences. McGraw-Hill, Inc., New York. 204–254.
35. Harling, O. K. 1969. Slow neutron inelastic scattering study of light water and ice. *J. Chem. Phys.* 50:5279–5296.
36. Pruppacher, H. R. 1972. Self-diffusion coefficient of supercooled water. *J. Chem. Phys.* 56:101–107.
37. Woessner, D. E., and B. S. Snowden. 1970. Pulsed NMR study of water in agar gels. *J. Colloid Interface Sci.* 34:290–299.
38. Brine shrimp elemental analysis by Schwarzkopf Analytical Laboratory, Woodside, New York.
39. Seitz, P. K., D. C. Chang, C. F. Hazlewood, H. E. Rorschach, and J. S. Clegg. 1981. The Self-Diffusion of Water in Artemia Cysts. *Arch. Biochem. Biophys.* 210:517–524.
40. Tanner, J. E. 1980. NMR measurements of self-diffusion in cells. *Fed. Proc.* 39:1758.
41. Tanner, J. E. 1983. Intracellular diffusion of water. *Arch. Biochem. Biophys.* 224:416–428.
42. Copley, J. R. D. 1974. Monte Carlo calculation of multiple scattering effects in thermal neutron scattering experiments. *Comp. Phys. Comm.* 7:289–317.
43. Copley, J. R. D. 1978. Institut Laue Langevin Report 78C0163T. 38042 Grenoble, France.
44. Clegg, J. S., S. Szwarnowski, V. McClean, R. J. Sheppard, and E. H. Grant. 1982. Interrelationships between water and cell metabolism in Artemia cysts. X. Microwave dielectric studies. *Biochim. Biophys. Acta.* 721:458–468.
45. Hasted, J. B. 1972. Liquid water: dielectric properties. Water. F. Franks, editor. Plenum Publishing Corp., New York. Vol. 1. 255–305.
46. Pennock, B. E., and H. B. Schwan. 1969. Further observations on the electrical properties of hemoglobin-bound water. *J. Phys. Chem.* 73:2600–2610.
47. Schwan, H. B. 1965. Electrical properties of bound water. *Ann. NY Acad. Sci.* 125:344–354.
48. Harvey, S. C., and P. Hockstra. 1972. Dielectric relaxation spectra of water adsorbed on lysozyme. *J. Phys. Chem.* 76:2987–2994.
49. Schwan, H. P., and K. R. Foster. 1977. Microwave dielectric properties of tissue. Some comments on the rotational mobility of tissue water. *Biophys. J.* 17:193–197.
50. Seitz, P., C. F. Hazlewood, and J. Clegg. 1980. Proton magnetic resonance studies on the physical state of water in *Artemia* cysts. *In* The Brine Shrimp Artemia. Physiology, Biochemistry and Molecular Biology. G. Persoone, P. Sorgeloos, O. Rolls, and E. Jaspers, editors. Universa, Wetteren, Belgium. 2:545–555.
51. Bloembergen, N., E. M. Purcell, and R. V. Pound. 1948. Relaxation effects in nuclear magnetic resonance absorption. *Phys. Rev.* 73:679–712.
52. Berendsen, H. J. C. 1962. Nuclear magnetic resonance study of collagen hydration. *J. Chem. Phys.* 36:3297–3305.
53. Clegg, J. S. 1982. Alternative views on the role of water in cell function. *In* Biophysics of Water. F. Franks, editor. John Wiley & Sons, Inc., New York. 365–383.